Article

Journal of the Brazilian Chemical Society

https://dx.doi.org/10.21577/0103-5053.20230175

J. Braz. Chem. Soc. **2024**, *35*, 5, e-20230175, 1-12
©2024 Sociedade Brasileira de Química

Synthesis and Characterization of Polyester Derived from Glycerol and Its Application as an Adhesive on Different Adherents

Érica L. de Oliveira,[a] Maísa B. Costa,[b] Luciana M. Ramos[b] and Olacir A. Araújo[*,a]

[a]*Laboratório de Química de Materiais e Modelagem Molecular (QMMOL), Universidade Estadual de Goiás, Campus Central, SEDE-CET, 75132-903 Anápolis-GO, Brazil*

[b]*Laboratório de Química Medicinal e Síntese Orgânica (LaQuiMeSO), Universidade Estadual de Goiás, Campus Central, SEDE-CET, 75132-903 Anápolis-GO, Brazil*

With the increase in the supply of glycerol and its economic devaluation, it is important to develop strategies that add value to this substance. Among the various alternatives, one application is its use as a precursor in the synthesis of new polyesters. Therefore, this work describes the condensation reaction of glycerol with valeric acid, obtaining functionalized glycerol, which was used in the polycondensation reaction with terephthalic acid. The samples were characterized by infrared spectroscopy, thermogravimetric analysis, hydrogen nuclear magnetic resonance and differential scanning calorimetry. Spectroscopic analyses confirmed the conversion of the reagents into esters and polyesters. The polyesters showed superior thermal stability than the individual components, a glass transition temperature of −3.8 °C and adhesive properties on glass, wood, paper and rigid polyvinyl chloride substrates. The adhesive capabilities of the samples were compared with those of commercial adhesives already established in the Brazilian market. Samples of polyesters synthesized through the reaction between functionalized glycerol and terephthalic acid showed adhesive behavior in the range of mechanical resistance observed in commercial adhesives, with an elastic modulus ranging from 60.9 ± 36.0 MPa to 162.1 ± 102.4 kPa, depending on the type of adhesive substrate, behaving either as an elastic and/or thermoplastic adhesive.

Keywords: polycondensation, polymers, residue, adhesive, functionalization

Introduction

In a scenario of a depletion of oil reserves aggravated by environmental pollution, in part with fossil fuels, renewable energy sources, especially biofuels, have been gaining attention.[1,2] A biofuel that has stood out in this area is biodiesel, which is produced from vegetable and animal oils through esterification reactions.[1-5] This process results in a product similar to conventional diesel, of which glycerol is the main by-product, constituting about 10% of the total production mass.[2,3,5-10] Thus, it is important, and of economic interest, the development of strategies that convert the biodiesel co-produced glycerol into a product with greater added value.[3,10]

Growing concern about environmental issues has led to the study and development of alternative and environmentally safe routes for the production of synthetic polymers, which are widely used today.[11] In this context, glycerol-derived polyesters stand out, as they are versatile polymeric materials in terms of properties, since they are biodegradable, are obtained from a renewable source and it is possible to adjust their mechanical and chemical properties depending on the synthesis conditions and precursors.[12-14]

Glycerol (compound **1**) is composed of trifunctional molecules for polycondensation reactions, belonging to the group of alcohols and, therefore, presents characteristics of reacting with dicarboxylic acids to form polyesters.[15] The literature reviewed in this article refers to research based on the use of glycerol or its derivatives as precursors in the synthesis of polyesters that can be applied in different areas such as biomedical, composites, fuel additives, flame retardant and adhesives, among others.[15-29]

In adhesion science and technology, the materials to be bonded are called adherent substrates. Gluing is the surface-to-surface joining of similar or dissimilar materials using a substance that is usually of a different type, called adhesive,

*e-mail: olacir.araujo@ueg.br
Editor handled this article: Hector Henrique F. Koolen (Associate)

This is an open-access article distributed under the terms of the Creative Commons Attribution License.

which adheres to the surfaces of the two adherends to be joined, transferring the forces from one adherent to the other. It is a technique of joining materials that, in the traditional sense, cannot be broken without destroying the bond.[30,31]

An adhesive is a non-metallic substance capable of joining materials by surface bonding (adhesion), and this connection has adequate internal resistance (cohesion, that is, an attraction between atoms or molecules of the same substance).[30,31] Adherents are usually in a solid state, while adhesives can be in a solid or liquid state. There are a wide variety of adherents and adhesives available, together with a variety of different processes for joining materials. This results in scientists specializing in a specific area of adhesion/adhesives. Examples of adherent materials include plastics, textiles, wood, tapes, coated abrasives, building materials, and materials used in the automotive and aerospace industries.[30,31]

One of the determining factors when selecting an adhesive for a given application is the glass transition temperature (T_g), since at temperatures above this the adhesive has a flexible appearance, which, in certain cases, can compromise the strength of the adhesive joint.[32] Thus, the principle of adhesion involves the insertion of an intermediate layer between the surfaces of the two parts to be joined. The intermediate layer must have sufficient internal mechanical strength (cohesion) and must be able to bond both surfaces of adherent substrates (adhesion). If the level of adhesion is inadequate, when put under tension, the adhesive layer separates from the surface to which it has adhered. If the level of cohesion is insufficient, fracture occurs in the adhesive layer. If two parts were perfectly glued together, then under stress, a fracture occurs within one of the parts, and not at the adhesive joint.[33]

An adhesive is a linear or branched amorphous polymer above its T_g (polymers that crosslink and are thermosetting are not included in this definition). It must be able to flow on a molecular scale to "grip" to adherent surfaces and is usually plasticized by the action of a solvent, which evaporates during the adhesion process.[34]

When it comes to the application of polymers as adhesives, it is important to consider the environmental and toxicological concerns currently discussed, thus, it is expected that the adhesives can be prepared from precursors from renewable sources, which are easy to acquire, economically accessible and non-toxic.[35-37]

In this sense, Zhang *et al.*[25] prepared hydrogels from methacryloyl-cytosine chloride (CMA), glycerol-polycaprolactone (GPCL) and *n*-butyl acrylate and acrylic acid (AAc). The mass proportions of CMA were varied relative to the AAc in 0, 0.06, 0.12 and 0.18 and their adhesive capacity on glass, stainless steel, polypropylene, wood, ceramics, rubber, polyethylene terephthalate, polytetrafluoroethylene and pigskin were evaluated. The explanation for the adhesive property considered the existence of a variety of functional groups such as C=O, NH_2, C=N and C–N, hydrogen interactions and complexation with the metal, specifically iron. The material with a proportion of 0.06 showed better adhesion to glass, while the one with a proportion 0.12 showed better adhesion to stainless steel.

In this context, this work is justified by the need to develop strategies that transform biodiesel co-produced glycerol into a product with greater added value. As a rule, precursor diols originate polyesters of linear aliphatic chains with greater elasticity, while triols and polyols result in polyesters of branched or cross-linked chains, more rigid, with greater mechanical, thermal, chemical resistance and materials with greater durability.[38,39] As glycerol is a trifunctional alcohol, with the aim of obtaining a linear polymer, the condensation reactions of this compound with valeric acid (compound **2**) were investigated, with the aim of deactivating one of the hydroxyls groups and producing the chemical species named "glycerol functionalized with valeric acid (GFAV)" (compound **3**). Valeric acid was chosen because it has a chemical structure with a short carbon chain, which can reduce the steric hindrance in glycerol polycondensation reactions. The subsequent step aimed to investigate the polycondensation reactions between GFAV and terephthalic acid, forming the polyester called GFAV_TA (glycerol functionalized with valeric acid and terephthalic acid) and its application as an adhesive in different adherents.

Experimental

The reagents and solvents used were all analytical grades. Glycerol (compound **1**) was purchased from Dinâmica (Indaiatuba, Brazil), valeric acid (compound **2**) and terephthalic acid (compound **4**) were purchased from Sigma-Aldrich (Saint Louis, USA). Nafion 417® was purchased from Sigma-Aldrich (Saint Louis, USA), infrared grade KBr, deuterated chloroform ($CDCl_3$) and tetramethylsilane (TMS) were purchased from Sigma-Aldrich (Darmstadt, Germany), ethyl acetate purchased from Neon (Suzano, Brazil). The products of the synthesis are numbered as follows: GFAV (glycerol functionalized with valeric acid, compound **3**) and GFVA_TA (glycerol functionalized with valeric acid and terephthalic acid, compound **5**).

Functionalization of glycerol (compound **1**) with valeric acid (compound **2**)

The functionalization reaction between compound **1** with compound **2** was carried out in a 0.5 L Kettle-type reactor coupled to a Dean Stark tube and ball condenser. To homogenize the temperature, a mechanical stirrer (Fisatom 713D, São Paulo, Brazil) was used, to which a glass rod and Teflon propeller were connected. To monitor and control the temperature of the reaction system, a temperature controller Novus N1200 (Canoas, Brazil) and a 500 mL heating mantle Exodus (Hortolândia, Brazil) were used. 30 mL of compound **1** (0.41 mol) and 0.41 mol of compound **2** were added to the reactor. Nafion 417® was used as catalyst, which is a perfluorinated membrane reinforced with sulfonated polytetrafluoroethylene (PTFE). Subsequently, the system was maintained at 130 °C for 210 min. Water, by-product of the reaction, collected in the Dean Stark tube, was used as a parameter to identify the beginning and end of the reaction.

Polycondensation of GFAV (compound **3**) with terephthalic acid (compound **4**)

The polycondensation reaction of compound **3** with compound **4** was carried out in the same reaction system as the functionalization reactions, with the addition of 0.41 mol of compound **4** and Nafion 417®. Then, the system was heated at 190 °C for 210 min and the product was named GFVA_AT.

Characterizations

Infrared spectra (FTIR)

Infrared spectra were collected on a Spectrum Frontier FT-IR MID-NIR PerkinElmer spectrometer (Waltham, USA), in the mid-infrared region (4000-400 cm^{-1}) at the Center for Analyses, Innovation and Technology in Natural and Applied Sciences at Goiás State University (UEG)-CAITEC. Samples were dispersed in KBr and pressed into pellets.

Thermogravimetric analysis (TGA)

Thermogravimetric analyses were performed using Pyris 1 TGA PerkinElmer (Waltham USA) equipment at the Center for Analyses, Innovation and Technology in Natural and Applied Sciences at Goiás State University (UEG)-CAITEC. Temperature ranges from 25 to 500 °C and 25 to 700 °C were used, both at a heating rate of 10 °C min^{-1} and nitrogen gas flow at 20 mL min^{-1}.

Nuclear magnetic resonance (NMR)

A Bruker Avance III 500 MHz spectrometer was used for ^1H nuclear magnetic resonance (NMR), 11.7 T (Karlsruhe, Germany), with ATB (Automation Triple Resonance Broadband) and SW (switchable) probes, 5 mm internal diameter, at room temperature and pulse of 45 ºC for hydrogen and carbon, at the Institute of Chemistry at the Samambaia Campus of the Federal University of Goiás (IQ/UFG). Chemical shifts (δ) in ^1H NMR with deuterated chloroform with tetramethylsilane ($CDCl_3$/TMS) were purchased from Sigma-Aldrich (Saint Louis, USA). Multiplicities were defined in the usual way, s (singlet), d (doublet), dd (double doublet), t (triplet), q (quartet), qu (quintet), m (multiplet).

Differential scanning calorimetry (DSC)

The physical transitions of the polycondensation products were monitored in the PerkinElmer DSC 400 equipment (Waltham, USA), in the temperature range from −100 to 170 °C in a nitrogen atmosphere at 20 mL min^{-1}, at the Center for Analyses, Innovation and Technology in Natural and Applied Sciences at Goiás State University (UEG)-CAITEC. Initially, a sample of approximately 10 mg was submitted to 1 min of isotherm at 25 °C. Then, cooling was carried out from 25 to −100 °C and subsequently heated from −100 to 170 °C, both at 5 °C min^{-1}. Data were collected from this third step.

Application of GFVA_TA (compound **5**) as adhesive

Adhesive formulation

Compound **5** is a material with the physical appearance of a rubbery solid at room temperature, and it is necessary to apply it through dispersion in liquid solvent. The choice of solvent must take into account, in addition to availability, the solvent associated with less toxicity, which is more economically accessible and volatile.[40] Thus, among the solvents in which compound **5** was soluble, ethyl acetate was selected to prepare the adhesive mixture. The dispersion concentration was 157.9 g L^{-1} and was packaged in a polypropylene bottle. Adhesion tests were carried out on wood, glass and paper substrates and rigid PVC (polyvinyl chloride) joints.

Test specimens preparation

In order to determine the adhesive capacity of GFAV_TA, shear tests were carried out using the standard ASTM (American Society for Testing and Materials) 1002[41] which was adapted for testing on wood and glass. The specimens made of Guatambú wood (*Balfourodendron riedelianum*) and glass were prepared

according to dimensions of 120 mm in length, 26 mm in width and 4 mm in thickness. The glass was cleaned with ethanol and paper towels before application. The wood was used without prior treatment. In each tensile test, two specimens of the same material were used, glued to each other by means of the adhesive mixture. Bonding was performed by spreading the adhesive mixture over an area of 3.302 cm^2 from the edge of each specimen (1.27 cm from the edge), which were joined and kept under pressure for 60 min. For comparison purposes, two commercial wood adhesives based on polyvinyl acetate, from different brands, and two commercial glass adhesives, one based on silicone and the other based on silane and hydrocarbon resin were used. The application conditions of the commercial adhesives were the same as those used for compound **5**. For paper adhesion tests on wood and glass substrates, an adaptation was made to the ASTM 4862 standard.[42] A4 paper tapes, grammage 75, 100 mm in length and 26 mm in width were used. The adhesive mixture was applied between the paper and the substrate in an area of 5.2 cm^2, which corresponds to 20 mm from the edge of the paper tape, maintaining it under pressure for 5 min. The paper was superimposed on the wood without any previous treatment, and the glass was cleaned with ethanol. The tensile tests were carried out with the paper tape making an initial angle of 90º with the substrates. Tests were carried out with the adhesive mixture of compound **5**, and with the commercial adhesives for wood and glass that showed better adhesion power. Figure 1 shows the photographs of some specimen tests.

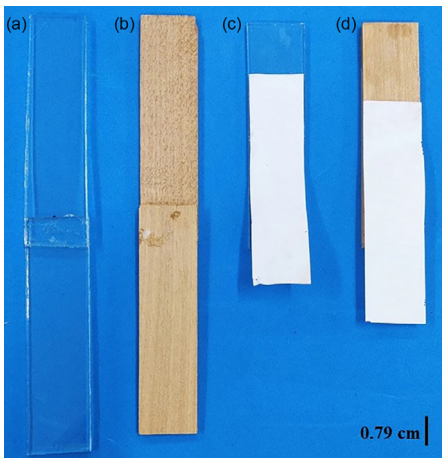

Figure 1. Photograph of specimens bonded with a mixture of compound **5**: (a) glass, (b) wood, (c) paper on glass and (d) paper on wood.

Mechanical tests

The tensile tests were carried out in a universal mechanical testing machine Emic model DL 2000 (São José dos Pinhais, Brazil). The ends of the wood/wood and glass/glass specimen tests were fixed in the machine's grips, so that each grip was adjusted to 63.5 mm of overlapping area. The tests were carried out using a load cell of 5000 N, at a speed of 1.3 mm min^{-1}, and the maximum tensile strength and modulus of elasticity were recorded. Tests were performed on ten specimen tests for each sample. In the tensile test of paper glued to wood or glass, the glass or wood substrate was fixed to the base of the machine with the aid of two 2-inch C-type metal clamps. The paper was gripped in the upper grip 63 mm from the base of the wood or glass substrate. In this tensile test, the flexible adherent (paper) is removed from the rigid adherent (wood or glass) at a rate of 10 mm min^{-1} with an initial angle of 90º between the tape and the rigid adherent. The test was performed using a 50 N load cell and the maximum tensile strength and modulus of elasticity were recorded. Tests were performed on ten specimens of each sample.

Results and Discussion

Infrared spectra (FTIR)

The functionalization product between glycerol (compound **1**) and valeric acid (compound **2**) called GFVA (compound **3**), presented characteristics of a viscous liquid and odor of compound **2**. Figure S1 (Supplementary Information (SI) section) presents the FTIR spectra of compounds **1**, **2** and **3** and Table S1 (SI section) presents the assignments of the main absorption bands. It is observed that the C=O stretching band was shifted from 1703 cm^{-1} in the compound **2** spectrum to 1739 cm^{-1} in the compound **3** spectrum, which shows the formation of the ester group, confirming the esterification reaction. However, a weak absorption is observed at 1706 cm^{-1} (shoulder), which was attributed to the C=O stretching of the carboxylic acid, indicating the presence of some unreacted acid. Furthermore, it is observed that the intensities of the O–H stretching band of alcohol at 3756-3068 cm^{-1} and angular deformation at 1645 cm^{-1}, in the spectrum of glycerol, decreased in the spectrum of **3** when compared to the intensities of the C–H stretching bands (2944 cm^{-1}) in both spectra. This behavior suggests a decrease in the proportion of O–H groups in compound **3**, which is consistent with the formation of ester groups. The relative intensity of the peaks at 1106 and 1047 cm^{-1}, corresponding to C–O stretching vibration of hydroxyl on secondary and primary carbons respectively, can also be used as a reference to monitor the occurrence of esterification in the glycerol molecule. There are two primary and one secondary carbon in the glycerol molecule, which results in a more intense absorption peak at 1047 cm^{-1} than at 1106 cm^{-1}. The FTIR analyzes were

performed qualitatively, therefore, the comparison of the intensity of the bands between different spectra would result in an erroneous interpretation. However, when comparing the relative intensity of the bands in the same spectrum, it is possible to verify whether that sample has a greater amount of primary than secondary hydroxyls. It is observed in the spectrum of compound **3**, compared to glycerol spectrum that the peak intensity at 1047 cm^{-1} decreased in relation to the absorption at 1106 cm^{-1}, which indicates a decrease in the amount of primary hydroxyls in relation to secondary ones.[19] This result suggests that the functionalization of glycerol occurred preferentially in the primary (terminal) hydroxyls, which causes the appearance of steric hindrance in the secondary hydroxyl.[15] Scheme 1 shows the proposed functionalization reaction of compound **1** with compound **2**, forming compound **3**.

The GFVA_TA (compound **5**) polyester obtained from the polycondensation between compounds **3** and **4**, presented the characteristic of a rubbery solid. Figure S2 (SI section) shows the FTIR spectra of compounds **4**, **5** and, for comparative purposes, compound **3**. The main wavenumbers and their assignments are described in Table S2 (SI section). The absorption band at 1739 cm^{-1}, attributed to the C=O stretching of ester groups, associated with a decrease in the relative intensity of the absorption at 937 cm^{-1}, corresponding to the out-of-plane angular deformation C–O–H in carboxylic acid, and absence of the O–H stretching band of alcohol and carboxylic acid in the **5** spectrum, indicate that the hydroxyl groups of compound **3** reacted with compound **4** with the formation of ester groups, which confirms the occurrence of polycondensation reactions.[27,36,43,44] However, absorption at 1684 cm^{-1} (shoulder) was observed, a characteristic of C=O stretching of carboxylic acid. This absorption suggests the presence of unreacted acid or terminal carboxylic groups of the formed polymeric chain.[17,18,25] Thus, the absorptions at 1684 and 937 cm^{-1} were attributed to the end groups of the polyester molecules, since the thermal behavior of the polyester, determined by thermogravimetry, did not indicate the presence of residual compound **4**. Scheme 2 shows the proposed polycondensation reaction of compounds **3** and **4**, forming compound **5**.

Thermogravimetric analysis (TGA)

The thermal behavior of all five compounds **1**, **2**, **3**, **4** and **5** are shown in Figures 2 and 3 through thermogravimetric curves and respective derivatives. The percentages and respective mass loss stages are shown in Table 1. It is observed that the thermal stability of compound **3** was greater than compound **2** (valeric acid) and less than compound **1** (glycerol). The intermediate thermal behavior of a product in relation to the reactants can indicate either the formation of a new chemical species, or a mixture of the reactants. Thus, the theoretical curve was calculated using the following procedure: each point of the experimental curve of compound **1** was multiplied by its percentage value or mass fraction (0.474). The same procedure was performed for the compound **2** curve (0.526). The values obtained were added, which originated the points of the theoretical curve, and assuming that there were no chemical interactions between the reactants in the blend during the thermal degradation in an inert atmosphere. The calculated curves are useful for comparison purposes with the experimental curves, as the effects of chemical interactions between the individual components of a mixture can be

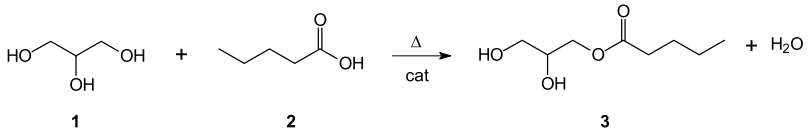

Scheme 1. Functionalization reaction proposal of glycerol (compound **1**) with valeric acid (compound **2**), forming GFVA (compound **3**).

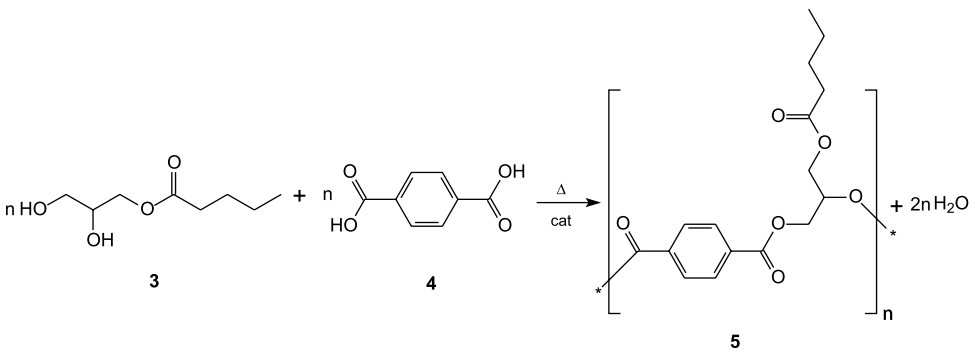

Scheme 2. Polycondensation reaction proposal of GFVA (compound **3**) and terephthalic acid (compound **4**), forming GFVA_AT (compound **5**).

analyzed using this comparison. The chemical interaction between the components of the mixture can accelerate or delay the decomposition process, and if there is no interaction, the calculated theoretical curve will present a similar profile to the experimental curve. The overlapping of the experimental curve with the theoretical curve means that each of the constituents decomposes independently, that is, there is no chemical interaction.[45]

Table 1. Temperatures and percentages of mass loss of samples analyzed by thermogravimetry

Compound	Steps and percentages of mass loss		
	1st / °C	2nd / °C	MDST / °C
1	140-255 (93)		246
2	46-167 (99)		160
3	30-112 (8)	112-260 (90)	247
4	260-383 (84)	383-425 (14)	372
5	160-350 (8)	350-545 (77)	450

MDST: maximum degradation speed temperature. Values in parentheses are the percentages.

It is observed that the experimental curve does not coincide with the theoretical curve, which suggests that compounds **1** and **2** are chemically bonded, with the formation of compound **3**. The intermediate thermal stability of the individual constituents is related to the esterification of compound **1** by compound **2**, because as the hydroxyl groups are functionalized, hydrogen bonds are replaced by van der Waals interactions associated with the carbon chain of compound **2**. The increase in molar mass is not enough to compensate the decrease in the intensity of intermolecular interactions. The thermogravimetric curves of compounds **1** and **2** show a mass loss step each. In compound **1**, the step occurred in the range of 140-255 °C, with 93% mass loss, and in compound **2** in the range of 46-167 °C, with 99% mass loss. The slopes of the curves show that the rate of mass loss occurs rapidly, indicating the existence of one or a few simultaneous thermal events, such as boiling.

In the compound **3** curve, two stages of mass loss were observed, which occurred in the ranges of 30-112 and 112-260 °C, with 8 and 90% of mass loss, respectively. The first stage was attributed to vaporization of residues of water (reaction by-product) and compound **2** by boiling and the second to vaporization of sample by boiling. These results are consistent with those obtained by FTIR, which indicated the presence of residues of compound **2**, and suggest that at least 92% of the sample corresponds to the GFVA product (compound **3**), being an estimate of the effectiveness of the reaction. Regarding the thermal behavior of compound **5**, it is observed that the thermal stability was greater than that of the individual constituents, which indicates the formation of a new chemical species, and can be explained by the increase in molar mass that occurs through the reaction between molecules of compounds **4** and **3**, which also resulted in increased intermolecular interactions. Two stages of mass loss are observed, the first occurred at 160-350 ºC, with 8% mass loss, and was attributed to vaporization of residual compound **3**. The second occurred in the range of 350-545 ºC, with 77% mass loss, and was attributed to boiling vaporization with simultaneous thermal degradation. These results are consistent with those obtained by FTIR and consistent with polyester samples, according to data from the literature.[15,38,46]

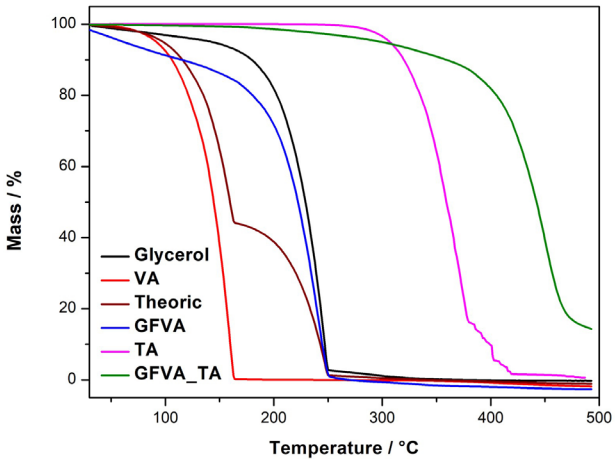

Figure 2. Thermogravimetric curves of compounds **1**, **2**, **3**, **4** and **5** and theoretical.

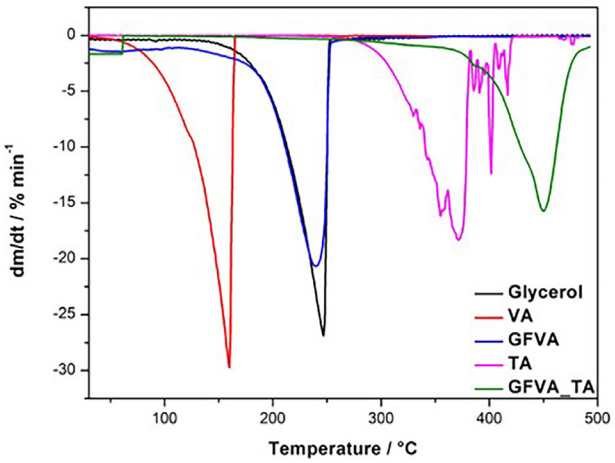

Figure 3. Derivatives of the thermogravimetric curves of compounds **1**, **2**, **3**, **4** and **5**.

Hydrogen nuclear magnetic resonance (^{1}H NMR)

Figure S3 (SI section) shows the ^{1}H NMR spectrum of compound **3** and the representation of the proposed

chemical structure. In the most shielded region, the triplet is observed at 0.92 ppm and an integral 3, which was assigned to the methyl group (A) at the end of the carbon chain. The multiplet in 1.34 ppm and 2 integral is characteristic of shielded methylene hydrogens (CH_2) (B). The quintet at 1.62 and integral 2 was attributed to the absorption of methylene hydrogens in β position to the carbonyl group (C), which shifted to a more shielded field due to the anisotropy effect of the adjacent C=O group of the ester. The quartet at 2.36 ppm and integral 2 was attributed to methylene hydrogens in the α position in relation carbonyl (D), unshielded due to greater proximity to the adjacent C=O group of the ester. The multiplet at 4.17 ppm with integral 2 was assigned to the methylene hydrogens of carbon bonded to oxygen (E), which are unshielded due to the electronegativity of oxygen. The doublet of doublet of doublets at 3.69 ppm and integral 2, corresponding to the methylene hydrogens of the terminal carbinolic carbon (G). The quintet at 3.95 ppm and integral 1 was assigned to the secondary carbon hydrogen (F). In the spectrum, the absorption peaks of hydroxyl hydrogens in the primary and secondary carbons were not observed, which present variable chemical shifts in the region between 0.5 and 5.0 ppm. This variation is dependent on sample concentration and solvent volume, temperature and presence of impurities. Furthermore, this variation may be related to the ability to exchange protons between these groups and the deuterium of $CDCl_3$. When this exchange occurs, the hydroxyl proton signal does not appear in the spectrum.[39,47] This effect also explains the absence of the signal corresponding to the hydrogen of the carboxylic group, present in residual from the compound **2**, which generally appears at approximately 12 ppm. The NMR results indicated the functionalization of a primary hydroxyl of glycerol by compound **2** with the formation of compound **3**, as proposed in the FTIR analysis.

Figure S5 (SI section) shows the ^{1}H NMR spectrum of compound **5** and the representation of the proposed chemical structure. The multiplet at 0.92 ppm was attributed to the methyl group (A) present at the end of the carbon chain. In the most shielded region of the spectrum, the multiplet at 1.34 ppm was attributed to the methylene hydrogens (B). The multiplet at 1.60 ppm was attributed to the methylene hydrogens (C) in the β position to the carbonyl, and the multiplet at 2.35 ppm to the methylene hydrogens (D) in the α position. These hydrogens are unshielded due to the anisotropy effect of the carbonyl group. There are signs of complex visualization in the most unshielded region, located in the range 4.71-4.18 ppm, which were attributed to the hydrogens (F) in the carbons between two ester groups. These hydrogens are unshielded due to the electronegativity of the oxygen atom, which acts as an electron withdrawer, facilitating resonance. This same effect explains the multiplet at 5.69 ppm, which was associated with hydrogen (G). This hydrogen feels the effect of electronegativity caused by the proximity of three electron-withdrawing groups present in its vicinity, that is, the oxygens of the ester groups. The multiplet at 8.08 ppm was attributed to the hydrogens of the aromatic ring (H), which are unshielded by the anisotropic field present in the ring.[45] The FTIR analysis detected the presence of carboxylic groups, which were associated with end groups of the polymeric chain. However, the absorption of hydrogen from this group, which should occur at approximately 12 ppm, was not observed. This effect, as already mentioned, can be explained by the possibility of exchanging this hydrogen with the deuterium in the solvent. The results do not show evidence of residual compound **3** in the analyzed sample.

Differential scanning calorimetry (DSC)

Figure 4 shows the DSC thermogram of compound **5**. The glass transition temperature (T_g) corresponds to the temperature at which the amorphous portion of a semi-crystalline polymer has enough energy to promote the mobility of the polymeric chains. In this way, the mechanical characteristic of the polymer is modified from a glassy and rigid aspect, at a temperature below the T_g, to a flexible one, at a temperature above the T_g.[48] The compound **5** showed a T_g at −3.8 ºC, a thermal event corresponding to a second-order transition and identified by the change in the baseline of the curve. The endothermic peak at 45.6 °C corresponds to the melting of the crystalline regions in the polymeric material. An exothermic peak was observed at 85 ºC which suggests the formation of

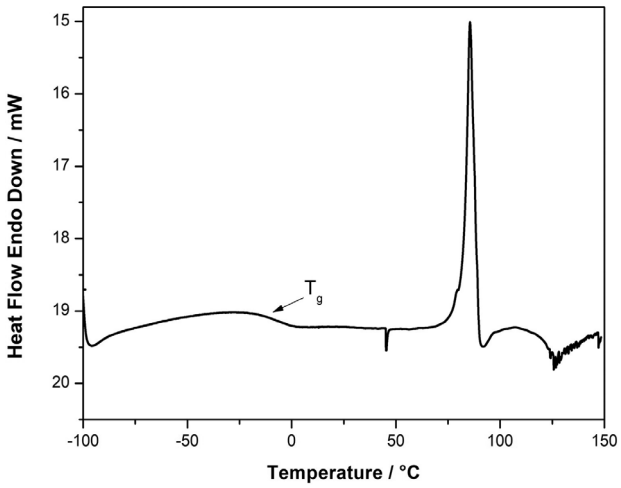

Figure 4. DSC curve of compound **5**.

chemical bonds associated with chain growth reactions of polymeric molecules. The endothermic peak at 126.6 °C was attributed to the vaporization of residual water from the polycondensation reaction.

Tensile tests using compound **5** as adhesive

The tensile test corresponds to the application of a force to a certain area of the specimen, causing its deformation.[49] The tests were carried out adapting the ASTM D1002 standard[41] for tensile tests on wood and glass adhesive joints, and adapting to the ASTM D6862 standard[42] for the tensile tests of paper glued to wood and paper glued to glass. The tests were carried out in a comparative way with commercial adhesives, evaluating the maximum tensile strength and modulus of elasticity (Young modulus). The stress corresponds to the force applied *per* unit area and, therefore, the maximum stress corresponds to the maximum force that can be applied to the specimen until its mechanical failure occurs. In adhesive joints, failure can occur in cohesion in the adhesive or substrate, or failure of adhesion between the adhesive and the substrate.[49-51] Maximum stress is a parameter used to evaluate the adhesion characteristics of an adhesive joint, as it will be related to its maximum strength.[52] The elastic modulus indicates the material's resistance to elastic deformation. Thus, materials can be classified according to the elastic modulus value when subjected to traction, so those with low elastic modulus are considered flexible and easily stretched, while those with high elastic modulus are rigid.[49,53] Regarding adhesives, this parameter is related to the type of application used. Adhesives that have a high modulus can be used in structural applications, which require sealants that are more rigid. Adhesives with low modulus, because they are more elastic, can be used in applications that require high movement capacity.[54]

Figures 5, 6 and 7 show, respectively, the bar graphs of maximum tensile strength and elastic modulus, with the respective standard deviations, and the stress *vs*. strain curves of the tensile tests of the wooden specimens glued with compound **5** and with the commercial stickers, for comparison purposes. The maximum tensile strength for compound **5** was 0.462 ± 0.215 MPa, 6.696 ± 1.484 MPa for commercial adhesive 1 (CA1) and 3.970 ± 0.934 MPa for commercial adhesive 2 (CA2). The elastic moduli were 60.9 ± 36.0 MPa for **5**, 364.5 ± 40.0 MPa for AC1 and 350 ± 46.0 MPa for AC2. These results indicate that compound **5** presents as an adhesive characteristic on wood, acting as an elastic adhesive.

Figures 8, 9 and 10 show, respectively, the bar graphs of maximum tensile strength and elastic modulus, with

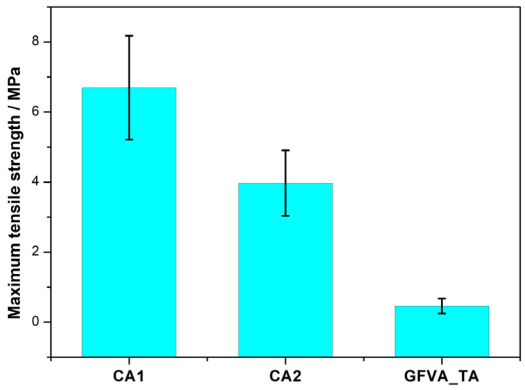

Figure 5. Maximum tensile strength of adhesive wood joints using compound **5** and commercial adhesives.

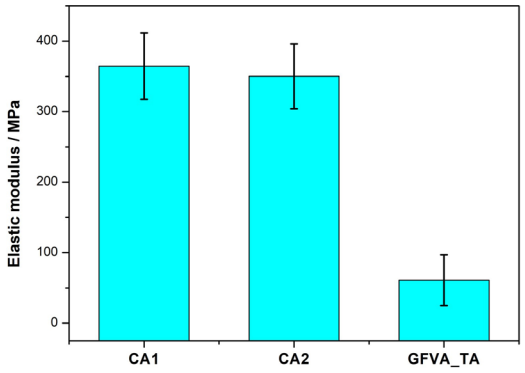

Figure 6. Elastic modulus of adhesive wood joints using compound **5** and commercial adhesives.

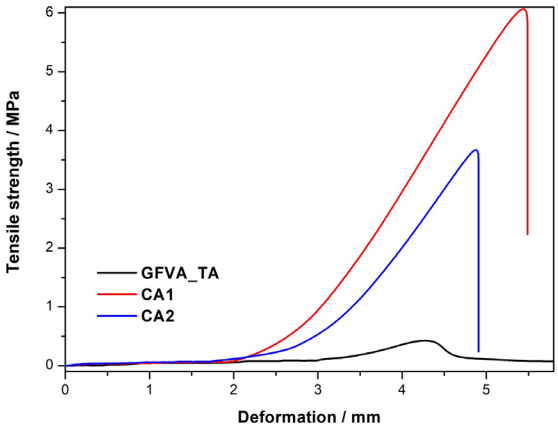

Figure 7. Stress *vs*. strain curves of adhesive wood joints using compound **5** and commercial adhesives.

the respective standard deviations, and the stress *vs.* strain curves obtained in the tensile tests of glass specimens prepared with compound **5** and commercial adhesives, for comparison purposes. The maximum tensile strength was 0.058 ± 0.019 MPa for compound **5**, 0.885 ± 0.176 MPa for commercial silicone-based adhesive (ACSilicone) and 0.735 ± 0.270 MPa for commercial silane-based adhesive (ACSilane). The elastic moduli values were 6.85 ± 11.2 MPa for compound **5**, 72.82 ± 55.7 MPa for ACSilicone and

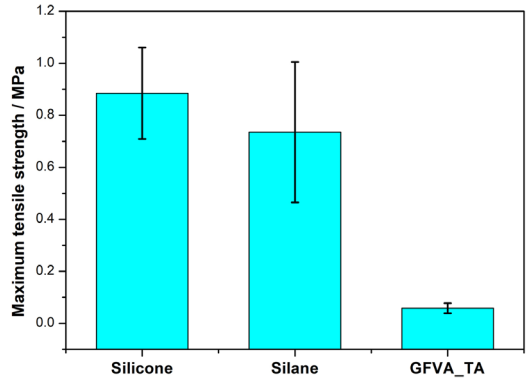

Figure 8. Maximum tensile strength of glass adhesive joints using compound **5** and commercial adhesives.

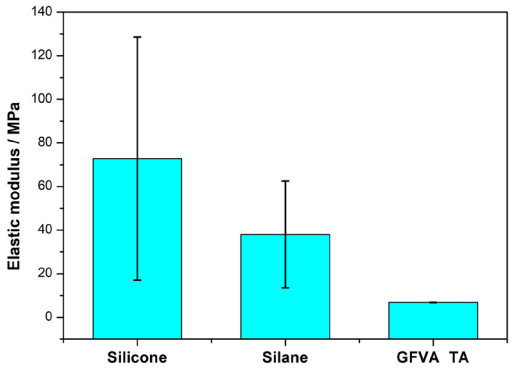

Figure 9. Elastic modulus of adhesive glass joints using compound **5** and commercial adhesives.

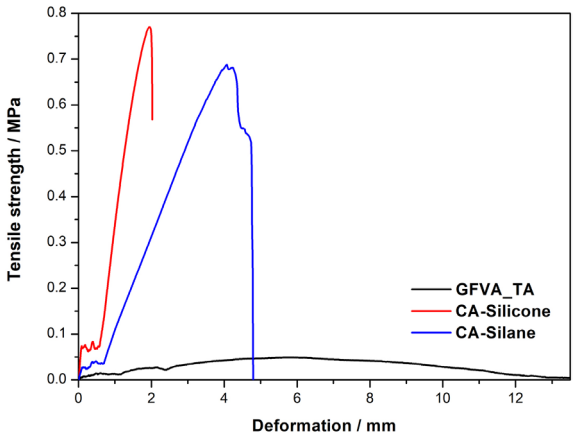

Figure 10. Stress *vs*. strain curves of glass adhesive joints using compound **5** and commercial adhesives.

38.03 ± 24.0 MPa for ACSilane. The results of maximum tensile strength and elastic modulus with commercial adhesives showed relatively high standard deviations when compared to the results obtained for compound **5**, indicating that the specimens bonded with compound **5** showed results with better repeatability, and that the adhesive layer showed less tendency to the appearance of defects in the bonding process. The stress *vs*. strain curve of compound **5**, as well as the visual observation, show that there was adhesive creep failure, indicating that compound **5** has adhesion properties on glass substrates with plastic behavior.

Figures 11, 12 and 13 show, respectively, bar graphs of maximum tensile strength and elastic modulus and their respective standard deviations, and stress *vs*. strain curves of adhesive joints of paper glued to wood using compound **5** as adhesive and comparing the results with CA1, for having greater adhesive strength on wood, and ACSilicone, for having greater adhesive strength for glass. In the tests carried out, the occurrence of failure in the paper substrate was observed, which is indicated by the behavior of the stress *vs*. strain curves. Paper tapes cut from the A4 paper sheets were used and, thus, these tapes may have different mechanical strength from each other. It was observed that in some tapes the rupture occurred only in the paper and in others in the part of the paper glued to the substrate. This behavior was the cause of such high standard deviations. The maximum stress values were 15.6 ± 4.7 kPa for compound **5**, 8.6 ± 2.8 kPa for AC1 and 16.1 ± 7.0 kPa for ACSilicone. These results show that this compound had the same adhesive performance as ACSilicone. The elastic moduli were 197.6 ± 124.9 kPa for compound **5**, 204.1 ± 198.5 kPa for CA1 and 80.1 ± 46.8 kPa for ACSilicone. These results indicate that the compound acts as an adhesive between paper and wood and that failure occurs in the paper substrate.

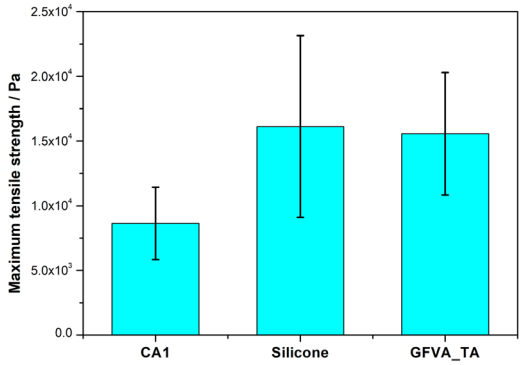

Figure 11. Maximum tensile strength of wood/paper adhesive joints using compound **5** and commercial adhesives.

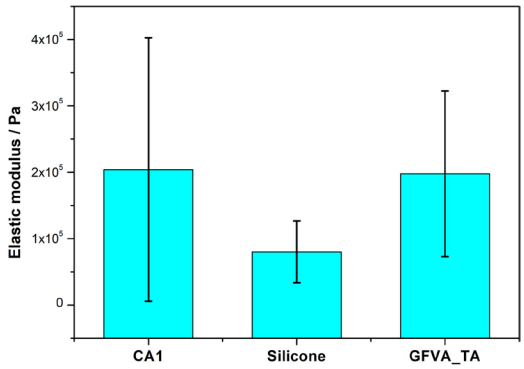

Figure 12. Elastic modulus of wood/paper adhesive joints using compound **5** and commercial adhesives.

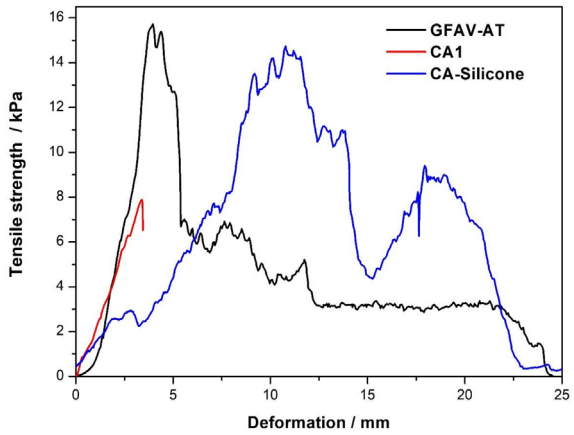

Figure 13. Stress *vs*. strain curves of wood/paper adhesive joints using compound **5** and commercial adhesives.

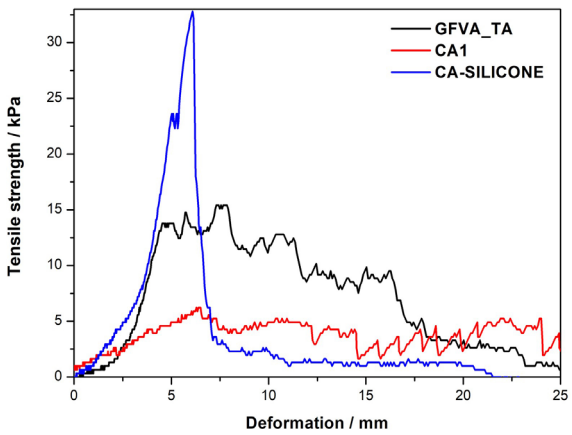

Figure 16. Stress *vs*. strain curves of glass/paper adhesive joints using compound **5** and commercial adhesives.

Figures 14, 15 and 16 show, respectively, bar graphs of maximum stress and elastic modulus and the respective standard deviations, and the stress *vs*. strain curves of adhesive joints of paper glued to glass using the compound **5**, CA1 and ACSilicone as adhesives. In the tests carried out, failure was recorded in the paper substrate, which is indicated by the behavior of the stress *vs*. strain curves. The maximum tensile strength values were 15.5 ± 3.4 kPa for compound **5**, 6.6 ± 2.6 kPa for CA1 and 30.7 ± 16.4 kPa for ACSilicone. It is observed that the results obtained with ACSilicone showed a relatively high standard deviation when compared with the results of the other samples, but it is not possible to state that the difference in the average values of maximum tensile strength of the samples with ACSilicone and compound **5** are statistically significant. The elastic moduli values were 162.1 ± 102.4 kPa for compound **5**, 48.4 ± 25.7 kPa for CA1 and 186.1 ± 95.0 kPa for ACSilicone. It was observed that the test results of the ACSilicone and the compounds' samples presented relatively high standard deviations, but it was not possible to determine that the respective mean values of the elastic modulus are statistically different. Comparing the results, it is observed that the adhesive capacity of compound **5** between paper and glass is similar to that of commercial adhesives.

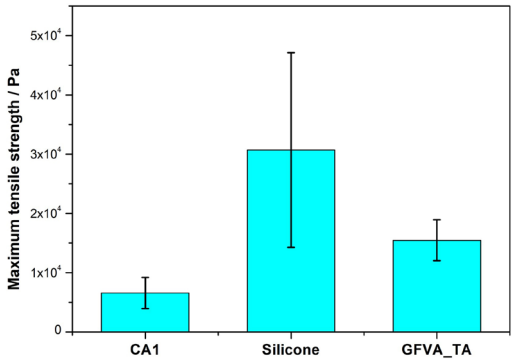

Figure 14. Maximum tensile strength of glass/paper adhesive joints using compound **5** and commercial adhesives.

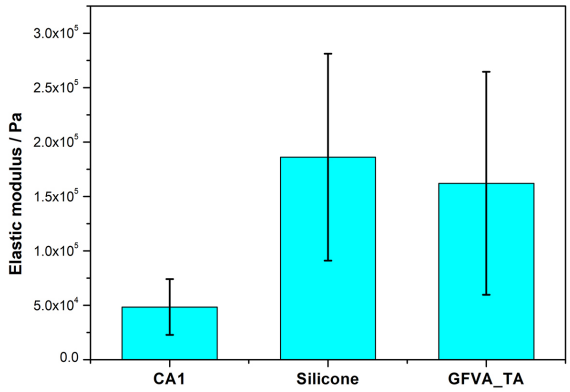

Figure 15. Elastic modulus of glass/paper adhesive joints using compound **5** and commercial adhesives.

Table 2 summarizes the maximum tensile strength and elastic modulus values of the specimens bonded with compound **5**. The highest values were obtained for wood and glass as adherent substrates. The lowest values, observed when bonding paper to glass and wood, may be related to the fact that the failure occurred in the paper substrate. The substrates were bonded by directly applying the dispersion of this compound in a solvent, without adding another type of adhesion additive to the mixture. It is noteworthy that an adhesive is rarely composed of only one polymeric class, since different materials with different properties can be combined in order to guarantee a synergistic effect to the adhesive, which occurs in the case of commercial adhesives.[31] The observed performance for compound **5** is adequate for its application as an adhesive for wood, glass and paper substrates. In addition to the quantitative results for these substrates, it was also observed, qualitatively, that the compound showed adhesive behavior for adherent substrates of ferrous metal sheets and PVC pipes and

Table 2. Maximum tensile strength and elastic modulus values of adhesive joints using compound **5** as adhesive

Property	Adherents			
	Wood / MPa	Glass / MPa	Paper and wood / kPa	Paper and glass / kPa
Maximum tensile strength	0.462 ± 0.215	0.058 ± 0.019	15.6 ± 4.7	15.5 ± 3.4
Elastic modulus	60.9 ± 36.0	6.85 ±11.2	197.6 ± 124.9	162.1 ± 102.4

connections. Figure 17 shows a photograph of pieces of ferrous metal, glass and wood glued together with a mixture of compound **5** as adhesive.

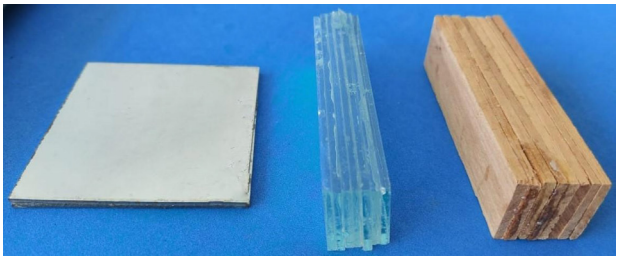

Figure 17. Photograph of pieces of ferrous metal, glass and wood bonded with the adhesive mixture of compound **5**.

Conclusions

Under the studied reaction conditions, it was possible to obtain compound **3** from the functionalization of compound **1** with compound **2**. Functionalized glycerol (compound **3**) showed adequate characteristics for polycondensation reactions with compound **4**, with formation of linear chain polyesters compound **5**. The T_g of the compound **5** polyester was –3.8 °C, which showed adhesive properties on adherent substrates of glass, wood, paper, ferrous metal sheets and PVC pipes and connections. The compound **5** polyester showed adhesive behavior in the range of mechanical resistance observed in commercial adhesives, with elastic modulus ranging from 60.9 ± 36.0 MPa to 162.1 ± 102.4 kPa, depending on the type of adherent substrate, behaving whether as an elastic and/or thermoplastic adhesive.

Supplementary Information

Supplementary information (Figures S1-S6 and Tables S1 and S2) is available free of charge at https://jbcs.sbq.org.br/ as a PDF file.

Acknowledgments

The authors would like to thank the Coordenação de Aperfeiçoamento de Pessoal de Nível Superior (CAPES) and Fundação de Amparo à Pesquisa do Estado de Goiás (FAPEG) for granting the scholarship. This project was financed through the "Universidade Estadual de Goiás/ Pró-projetos" program.

References

1. Budžaki, S.; Miljić, G.; Tišma, M.; Sundaram, S.; Hessel, V.; *Appl. Energy* **2017**, *201*, 124. [Crossref]
2. Farobie, O.; Matsumura, Y.; *Prog. Energy Combust. Sci.* **2017**, *63*, 203. [Crossref]
3. Ju, J.-H.; Heo, S.-Y.; Choi, S.-W.; Kim, Y.-M.; Kim, M.-S.; Kim, C.-H.; Oh, B. R.; *Bioresour. Technol.* **2021**, *337*, 125361. [Crossref]
4. Pradima, J.; Kulkarni, M. R.; Archna; *Resour.-Effic. Technol.* **2017**, *3*, 394. [Crossref]
5. Jo, M.-H.; Ju, J.-H.; Heo, S.-Y.; Cho, J.; Jeong, K. J.; Kim, M. S.; Kim, C.-H.; Oh, B.-R.; *Biotechnol. Biofuels Bioprod.* **2023**, *16*, 18. [Crossref]
6. Bueno, L.; Toro, C.; Martín, M.; *Chem. Eng. Res. Des.* **2015**, *93*, 440. [Crossref]
7. Khanday, W. A.; Okoye, P. U.; Hameed, B. H.; *Energy Convers. Manage.* **2017**, *151*, 472. [Crossref]
8. Lang, K.; Sánchez-Leija, R. J.; Gross, R. A.; Linhardt, R. J.; *Polymers* **2020**, *12*, 2969. [Crossref]
9. Rodrigues, P. R.; Silvério, T. A. B.; Druzian, J. I.; *Braz. Arch. Biol. Technol.* **2019**, *62*, e19170498. [Crossref]
10. Ao, S.; Alghamdi, L. A.; Kress, T.; Selvaraj, M.; Halder, G.; Wheatley, A. E. H.; Lalthazuala Rokhum, S.; *Fuel* **2023**, *345*, 128190. [Crossref]
11. Geeti, D. K.; Niranjan, K.; *Prog. Org. Coat.* **2019**, *127*, 419. [Crossref]
12. Goujard, L.; Roumanet, P.-J.; Barea, B.; Raoul, Y.; Ziarelli, F.; Le Petit, J.; Jarroux, N.; Ferré, E.; Guégan, P.; *J. Polym. Environ.* **2016**, *24*, 64. [Crossref]
13. Hazarika, D.; Karak, N.; *J. Appl. Polym. Sci.* **2018**, *135*, 46738. [Crossref]
14. Lee, X. Y.; Wahit, M. U.; Adrus, N.; *J. Appl. Polym. Sci.* **2016**, *133*, 44007. [Crossref]
15. Baharu, M. N.; Kadhum, A. A. H.; Al-Amiery, A. A.; Mohamad, A. B.; *Green Chem. Lett. Rev.* **2015**, *8*, 31. [Crossref]
16. Alptekin, E.; *Energy* **2017**, *119*, 44. [Crossref]
17. Chongcharoenchaikul, T.; Thamyongkit, P.; Poompradub, S.; *Mater. Chem. Phys.* **2016**, *177*, 485. [Crossref]
18. Conejero-García, Á.; Gimeno, H. R.; Sáez, Y. M.; Vilariño-

Feltrer, G.; Ortuño-Lizarán, I.; Vallés-Lluch, A.; *Eur. Polym. J.* **2017**, *87*, 406. [Crossref]

19. Dutra, G. V. S.; Araújo, O. A.; Neto, W. S.; Garg, V. K.; Oliveira, A. C.; Júnior, A. F.; *Mater. Chem. Phys.* **2017**, *200*, 204. [Crossref]
20. Pasma, S. A.; Daik, R.; Maskat, M. Y.; *J. Wood Chem. Technol.* **2018**, *38*, 445. [Crossref]
21. Unnisa, C. N.; Priya, V. H.; Chitra, S.; *J. Adhes. Sci. Technol.* **2019**, *33*, 2707. [Crossref]
22. Xu, Q.; Cao, W.; Xu, L.; Liu, Y.; Zhang, H.; Yin, T.; Li, T.; *J. Food Process. Preserv.* **2018**, *42*, e13829. [Crossref]
23. Wilson, R.; Divakaran, A. V.; Kiran, S.; Varyambath, A.; Kumaran, A.; Sivaram, S.; Ragupathy, L.; *ACS Omega* **2018**, *3*, 18714. [Crossref]
24. Zeng, F.; Yang, X.; Li, D.; Dai, L.; Zhang, X.; Lv, Y.; Wei, Z.; *J. Appl. Polym. Sci.* **2020**, *137*, 48574. [Crossref]
25. Zhang, X.; Wang, D.; Liu, H.; Yue, L.; Bai, Y.; He, J.; *Eur. Polym. J.* **2020**, *133*, 109741. [Crossref]
26. Svensson, I.; Butron, A.; Puyadena, M.; González, A.; Irusta, L.; Barrio, A.; *Polymers* **2023**, *15*, 1093. [Crossref]
27. Nakiou, E. A.; Lazaridou, M.; Pouroutzidou, G. K.; Michopoulou, A.; Tsamesidis, I.; Liverani, L.; Arango-Ospina, M.; Beketova, A.; Boccaccini, A. R.; Kontonasaki, E.; Bikiaris, D. N.; *Polymers* **2022**, *14*, 5028. [Crossref]
28. Liu, H.; Tang, Y.; Zhang, S.; Xu, X.; Yang, J.; *LWT--Food Sci. Technol.* **2023**, *182*, 114919. [Crossref]
29. Ghaffari-Bohlouli, P.; Golbaten-Mofrad, H.; Najmoddin, N.; Goodarzi, V.; Shavandi, A.; Chen, W. H.; *Synth. Met.* **2023**, *293*, 117238. [Crossref]
30. Gardner, D. J. In *Handbook of Adhesive Technology*, 3rd ed.; Pizzi, A.; Mittal, K. L., eds.; CRC Press: Boca Raton, USA, 2018, p. 3.
31. Brockmann, W.; Geiß, P. L.; Klingen, J.; Schröder, B.; *Adhesive Bonding Materials, Applications and Technology*; Wiley-VCH GmbH & Co. KGaA: Weinheim, Germany, 2009.
32. Ramírez, F. M. G.; Moura, M. F. S. F.; Moreira, R. D. F.; Silva, F. G. A.; *Fatigue Fract. Eng. Mater. Struct.* **2020**, *43*, 1307. [Crossref]
33. Koltzenburg, S.; Maskos, M.; Nuyken, O.; *Polymer Chemistry*; Springer: Garching, Germany 2016.
34. Sperling, L. H.; *Introduction to Physical Polymer Science*, 4th ed.; John Wiley & Sons: Bethlehem, USA, 2006.
35. Gu, W.; Li, F.; Liu, X.; Gao, Q.; Gong, S.; Li, J.; Shi, S. Q.; *Green Chem.* **2020**, *22*, 1319. [Crossref]
36. Jin, T.; Zeng, H.; Huang, Y.; Liu, L.; Yao, W.; Lei, H.; Shi, S.; Du, G.; Zhang, L.; *Polym. Test.* **2023**, *120*, 107974. [Crossref]
37. Hevilla, V.; Sonseca, A.; Echeverría, C.; Muñoz-Bonilla, A.; Fernández-García, M.; *Eur. Polym. J.* **2023**, *186*, 111875. [Crossref]
38. Vlase, G.; Bolcu, C.; Modra, D.; Budiul, M. M.; Ledeţi, I.; Albu, P.; Vlase, T.; *J. Therm. Anal. Calorim.* **2016**, *126*, 287. [Crossref]
39. Zhang, X.; Liu, H.; Yue, L.; He, J.; Bai, Y.; *Polym. Degrad. Stab.* **2019**, *167*, 130. [Crossref]
40. Shybi, A. A.; Varghese, S.; Maria, H. J.; Thomas, S. In *Handbook of Adhesive Technology*, 3rd ed.; Pizzi, A.; Mittal, K. L., eds.; CRC Press: Boca Raton, USA, 2018, p. 190.
41. ASTM1002: *Standard Test Method for Apparent Shear Strength of Single-Lap-Joint Adhesively Bonded Metal Specimens by Tension Loading (Metal-to-Metal)*, Philadelphia, 2019.
42. ASTM D4862: *Standard Test Method for90 Degree Peel Resistance of Adhesives*, Philadelphia 2021.
43. Nasiri, S. S.; Ahmadi, Z.; Afshar-Taromi, F.; *Int. J. Biol. Macromol.* **2023**, *245*, 125521. [Crossref]
44. Nasiri, S. S.; Ahmadi, Z.; Afshar-Taromi, F.; *Life Sci.* **2023**, *312*, 121203. [Crossref]
45. Waldman, W. R.; De Paoli, M. A.; *Polym. Degrad. Stab.* **1998**, *60*, 301. [Crossref]
46. Thi Le Bui, T.; Anh Nguyen, D.; Van Ho, S.; Thi Ngoc Uong, H.; *J. Appl. Polym. Sci.* **2016**, *133*, 43920. [Crossref]
47. Pavia, D. L.; Lampman, G. M.; Kriz, G. S.; Vyvyan, J. R.; *Introdução a Espectroscopia*, 4th ed.; Ccengage Learning: Washington, USA, 2010.
48. McKenna, G. B.; Simon, S. L. In *Handbook of Thermal Analysis and Calorimetry*; Gallagher, P. K., ed.; Elsevier: Akron, USA, 2002.
49. Beer, F. P.; Johnston, E. R.; Dewolf, J. T.; Mazurek, D. F.; *Mecânica dos Materiais*, 7th ed.; AMGH Editora Ltda: Porto Alegre, Brazil, 2015.
50. Florian, G.; Gabor, A. R.; Nicolae, C. A.; Iacobescu, G.; Stănică, N.; Mărăşescu, P.; Petrişor, I.; Leulescu, M.; Degeratu, S.; Gîngu, O.; Rotaru, P.; *J. Therm. Anal. Calorim.* **2018**, *134*, 189. [Crossref]
51. Orgilés-Calpena, E.; Arán-Aís, F.; Torró-Palau, A. M.; Orgilés-Barceló, C. In *Handbook of Adhesive Technology*, 3rd ed.; Pizzi, A.; Mittal, K. L., eds.; CRC Press: Boca Raton, USA, 2018, p. 607.
52. Gonçalves, D. C.; Sánchez-Arce, I. J.; Ramalho, L. D. C.; Campilho, R. D. S. G.; Belinha, J.; *J. Braz. Soc. Mech. Sci. Eng.* **2022**, *44*, 55. [Crossref]
53. Jones, D. R. H.; Ashby, M. F.; *Engineering Materials*, 1st ed.; Elsevier: Waltham, USA, 2019.
54. Klosowski, J. M. In *Handbook of Adhesive Technology*, 3rd ed.; Pizzi, A.; Mittal, K. L., eds.; CRC Press: Boca Raton, USA, 2018, p. 411.

Submitted: May 4, 2023
Published online: November 1, 2023